Published in final edited form as:
Int J Comput Assist Radiol Surg. 2011 January ; 6(1): 111–117. doi:10.1007/s11548-010-0485-9.

Image registration of pre-procedural MRI and intra-procedural CT images to aid CT-guided percutaneous cryoablation of renal tumors

Sota Oguro, **Kemal Tuncali**, **Haytham Elhawary**, **Paul R. Morrison**, **Nobuhiko Hata**, and **Stuart G. Silverman**
Department of Radiology, Brigham and Women's Hospital, Harvard Medical School, 75 Francis Street, Boston, MA 02115, USA

Abstract

Purpose—To determine whether a non-rigid registration (NRR) technique was more accurate than a rigid registration (RR) technique when fusing pre-procedural contrast-enhanced MR images to unenhanced CT images during CT-guided percutaneous cryoablation of renal tumors.

Methods—Both RR and NRR were applied retrospectively to 11 CT-guided percutaneous cryoablation procedures performed to treat renal tumors (mean diameter; 23 mm). Pre-procedural contrast-enhanced MR images of the upper abdomen were registered to unenhanced intra-procedural CT images obtained just prior to the ablation. RRs were performed manually, and NRRs were performed using an intensity-based approach with affine and Basis-Spline techniques used for modeling displacement. Registration accuracy for each technique was assessed using the 95% Hausdorff distance (HD), Fiducial Registration Error (FRE) and the Dice Similarity Coefficient (DSC). Statistical differences were analyzed using a two-sided Student's *t*-test. Time for each registration technique was recorded.

Results—Mean 95% HD (1.7 mm), FRE (1.7 mm) and DSC (0.96) using the NRR technique were significantly better than mean 95% HD (6.4 mm), FRE (5.0 mm) and DSC (0.88) using the RR technique ($P < 0.05$ for each analysis). Mean registration times of NRR and RR techniques were 15.2 and 5.7 min, respectively.

Conclusions—The non-rigid registration technique was more accurate than the rigid registration technique when fusing pre-procedural MR images to intra-procedural unenhanced CT images. The non-rigid registration technique can be used to improve visualization of renal tumors during CT-guided cryoablation procedures.

Keywords

Multi-modality image fusion; Cryoablation; Renal tumors; B-Spline; Non-rigid registration

Introduction

Percutaneous cryoablation of renal tumors has been guided by MRI, US, and more recently CT [1-3]. CT is often favored because it is more available than MRI, and unlike US, can be used to visualize fully the effects of freezing during the procedure [4,5]. Like most CT-guided interventions, percutaneous cryoablation uses unenhanced CT images, and as a

sota@bwh.harvard.edu .

result, some tumors may not be visible [6]. Even if the tumor is visible, its margins may be indistinct. Intravenous (IV) contrast material can be administered to enhance visualization of the tumor, but its effect are often transient, and do not last long enough to be useful throughout the procedure. Furthermore, patients with renal insufficiency may not be able to receive IV contrast material [7]. The lack of tumor visualization with unenhanced CT can lead to difficulty in determining where to position the cryoablation applicators that can result in either an ineffective ablation, or an ablation that involves too much normal renal parenchyma [8,9]. To assist with this problem the interventional radiologist often relies on a pre-procedure contrast-enhanced CT or MRI that depicts tumor margins and surrounding structures, including vascular anatomy. 'Image registration' is a technique that attempts to match and correlate two different image datasets, and in this study brings pre-procedural MR images and intra-procedural CT images into anatomical alignment. Once registration has been performed, the relevant information from both registered images can be combined to provide a 'fusion image' that can be useful in depicting renal tumors during CT-guided cryoablation.

Common techniques for fusing two sets of images include rigid registration and non-rigid registration. The rigid registration technique considers the target organs as if they were rigid objects and tries to align two different images taken at different times without considering the deformation of the organ [10-13]. More recently, non-rigid registration techniques which take into account the deformation of the organ have been proposed [14,15]. To aid the assessment of regional renal function, a non-rigid registration technique was used successfully to align the kidney and correct for motion during each acquisition of a 3D dynamic contrast-enhanced MRI sequence [15]. To our knowledge, neither rigid nor non-rigid registration techniques have been applied to the kidney to aid CT-guided cryoablation procedures.

The purpose of this study was to determine whether a non-rigid registration technique was more accurate than a rigid registration technique when fusing pre-procedural contrast-enhanced MR images to unenhanced CT images during CT-guided percutaneous cryoablation of renal tumors.

Materials and methods

Patient population and clinical setting

After IRB approval, a retrospective study of the pre-procedural and intra-procedural image datasets of 11 consecutive patients (mean age 66.5 years; range 49–81) who underwent CT-guided percutaneous cryoablation of renal tumors between February and April 2009 was performed. Informed consent was waived. Four tumors were in the right kidney and seven tumors were in the left. Six tumors arose from the anterior half of the parenchyma of the kidney, three at the junction between anterior and posterior halves, and two from the posterior half. Eight tumors were exophytic, two were central abutting the sinus fat, and one was mixed as it was both exophytic and abutted renal sinus fat [16]. Mean tumor diameter was 23 mm (range 5–38 mm). All tumors were proven to be renal cell carcinoma by percutaneous biopsy before the procedure.

Pre-procedural contrast enhancement MR images of the upper abdomen were obtained with a 1.5T scanner (GE SIGNA, GE Healthcare, Milwaukee, WI) in the supine position. The protocol included transverse, fat-suppressed T1-weighted dynamic imaging with three dimensional (3D) fast-acquisition multiple-excitation spoiled gradient recalled acquisition in the steady state sequence (TR/TE: 3.3–4.3/1.5–2.2 ms; flip angle 10°; slice thickness 5 mm; gap 2.5 mm; plane pixel size ranging from 0.63 to 0.78 mm, matrix 512 × 512, 80–104 slices, acquisition time from 20 to 33 s.) with an 8-channel torso surface coil taken 30, 60,

90, and 360 s after the IV administration of 0.2 ml/kg (range 11–20 ml) of gadolinium-based contrast material (Magnevist, Berlex Laboratories, Wayne, NJ).

Intra-procedural unenhanced CT scans were obtained at the beginning of the procedure with a 40-channel multi-detector row CT scanner (Sensation Open, Siemens Medical Solutions, Forchheim, Germany), using the following protocol: 0.6 mm collimation, 0.5 s/rotation, 120 kV, 168–398 mA,with a matrix size of 512 × 512, plane pixel size ranging from 0.46 to 0.62 mm, slice thickness of 3 mm. Patients were in the right posterior oblique (n = 2), right lateral decubitus (n = 5), or left lateral decubitus position (n = 4).

Non-rigid and rigid registration techniques

Contrast-enhanced MR images of the upper abdomen acquired at 90 s after intravenous administration and the intra-procedural unenhanced CT images were transferred to a computer workstation with four quad-core AMD Opteron 2.0 GHz processors and 16GB of RAM on a Fedora 10 Linux operating system. The rigid and non-rigid registration techniques were performed using open source software, 3D Slicer (http://www.slicer.org/), an image processing and visualization modular software package [17]. An initial rigid registration of the contrast-enhanced MR image and the unenhanced CT image was performed by an abdominal staff radiologist who manually aligned the outer contour of the kidney containing the tumor. This rigid registration was then followed by performing a non-rigid registration between the same images. To eliminate irrelevant voxels in the registration process and to reduce the number of voxels in the computations, the images were cropped to limit the field of view to approximately 1 cm beyond the renal contour. The kidney was segmented (contouring the outline of the kidney) on the CT and MR images, respectively, to produce masked data (assigning 0 intensity to the pixels external to the kidneys) that included only the relevant pixels in the similarity measurement, effectively removing extraneous tissues and background voxels (e.g., liver, adrenal gland, bone, and fat) [18]. Kidney segmentation was performed using an intensity-based threshold segmentation that provided an initial estimate of organ delineation, followed by manual correction by an abdominal staff radiologist. A 3D volumetric non-rigid registration technique that employs an “affine transformation” followed by a “Basis-Spline (B-Spline) transformation” was then used. The affine transformation models the global motion of the kidney, compensating for changes in scale and shear, while the B-Spline transformation created a free-form deformation [10,14]. The non-rigid registration technique we used included the affine and B-Spline registration both driven by maximization of mutual information using the Flecther-Reeves-Polak-Ribiere (FRPR) gradient-line-search optimization. The affine used 30 histogram bins and 50,000 pixels to calculate the mutual information metric, whereas the B-Spline used 100 histogram bins and 250,000 pixels. The B-Spline control grid was set to 5×5×5 [19]. This dual process (affine + B-Spline transformation) attempted to morph the pre-procedural MR images onto the intra-procedural CT images, and therefore compensated for any soft tissue deformation that occurred in the kidney between the two sets of images (Figs. 1 and 2).

Data analysis

Rigid registration and non-rigid registration were compared in this study. The non-rigid registration technique requires a preliminary rigid registration step. This rigid registration is performed mostly to accommodate the difference in definition of the coordinate systems used in CT and MRI. In CT, the origin of the patient-centric coordinate system (or RAS coordinate system) is at the top left and on the first slice of a set of slices; in MRI, it is at the center of the imaging volume. This compensation of the coordinate systems is followed by an alignment of anatomy. Without these two stages of manual rigid registration, the non-rigid registration could not correct the local image mismatching due to organ deformation

since the images would be completely misaligned due to different definition of their coordinate systems. Accuracy of the rigid and non-rigid registration techniques were quantified using three metrics for validation: 95% Hausdorff distance (HD) [20], fiducial registration error (FRE) [21] and Dice Similarity Coefficient (DSC) [22]. HD was calculated to evaluate the discrepancy of the renal contours from the registered kidneys. HD was defined as the maximum mismatch distance between two contours from registered kidneys (Fig. 3). To calculate HD, the edges of the segmented kidneys from each of the registered images were extracted. More formally, Hausdorff distance from set A to set B is a maxi–min function, defined as:

$$\mathrm{HD}(A,B) = \max_{a\in A}\{\min_{b\in B}\{d(a,b)\}\}$$

where *a* and *b* are points of sets A and B, respectively, and *d(a, b)* is the Euclidean distance between these points. Since HD is highly susceptible to outliers such as noise, the upper 5% of distance measures were disregarded and the 95 percentile distance (95% HD) was used to evaluate registration accuracy [20]. Perfect alignment would yield a 95% HD equal to 0 mm.

The FRE was calculated to show a better indication of the alignment of the internal structures of the kidneys and was defined as a distance error, after registration, between a pair of corresponding anatomical points in the pre-procedural and intra-procedural data sets which are not used in the registration process. Mean FRE is defined as,

$$\bar{FRE} = \frac{1}{n}\sum_{i=1}^{n}|T(r_{ai}) - r_{bi}|$$

where *i* is the fiducial index, *T* is transformation matrix which registers the MR image, r_a and r_b are the position of the fiducial point *i* in the MR and CT image coordinate system, respectively. Two such points in the kidney were identified by an abdominal staff radiologist: an upper- and lower-pole calyx. Perfect alignment would yield a FRE equal to 0 mm.

The DSC was calculated to measure the volumetric overlap between the segmented kidneys which were derived from the registered images. The DSC is defined as,

$$DSC(A,B) = \frac{2(A\cap B)}{(A+B)}$$

where *A* and *B* are sets of voxels identified as signal in each of the segmented images [23] (Fig. 3). In this study, *A* was the segmented kidney from the CT data and *B* was the segmented kidney from the registered MR images. A DSC value of 1 is perfect alignment of the two image datasets.

Mean values of 95% HD, FRE and DSC metrics were calculated for both the rigid registration and non-rigid registration techniques, respectively. Using a two-sided Student's *t*-test, statistically significant differences ($P < 0.05$) of mean values between the methods were reported.

In addition, a visual comparison of renal contours between CT images and registered MR images was performed. The renal contours from the MR images after rigid and non-rigid

registration technique were overlaid on the CT images to compare renal contours between registered MR and CT images.

Processing time

The times for computing the processing steps of the rigid and non-rigid registration techniques were recorded and tabulated. The time for the rigid registration technique included the manual registration. The time for the non-rigid registration technique included rigid registration, image cropping, segmentation for CT images, affine and B-Spline computations. The time for the rigid registration technique was included also in the time calculation for the non-rigid registration technique, since the non-rigid registration technique required a preliminary rigid registration of the images. Segmentation of the pre-procedural MR images was not included in the processing time, since it can be performed prior to the day of the ablation procedure.

Results

Mean 95% HD for the non-rigid registration technique (1.7 ± 0.4 mm) was significantly lower than the mean 95% HD for the rigid registration technique (6.4 ± 4.4 mm) ($P < 0.05$). Mean FRE for the non-rigid registration technique (1.7 ± 1.1 mm) was significantly lower than the mean FRE for the rigid registration technique (5.0 ± 2.2 mm) ($P < 0.05$). Mean DSC value after the non-rigid registrations (0.96 ± 0.01) was significantly higher than the mean DSC for the rigid registrations (0.88 ± 0.04) ($P < 0.05$) (Fig. 4).

On visual inspection, the renal contours were matched better when the non-rigid registration technique was used than when the rigid registration technique was used. In addition, the full extent of the tumor could be seen with the fused images (Figs. 1 and 2).

Mean time to complete the rigid registration technique was 5.7 ± 1.3 min. Mean time for non-rigid registration technique was 15.2 ± 3.2 min. Mean computation time for affine and B-Spline registration was 9.4 and 39.0 s, respectively.

Discussion

Although, pre-procedural contrast-enhanced MRI and intra-procedural unenhanced CT images were successfully registered and fused in all cases, the non-rigid registration technique proved to be more accurate than the rigid registration technique. As detailed in the introduction, tumor margins are often not visualized on unenhanced CT images. Therefore, it is difficult to determine where to position the cryoablation applicators. This difficulty can result in either an ineffective ablation, or an ablation that involves too much normal renal parenchyma. Our registration technique may be useful in depicting renal tumors for planning the interventional approach, facilitating the safe placement of the ablation applicators in the tumor, and monitoring the ablation effects during cryoablation. These unmet needs motivated the development of this registration technique. However, the purpose of our study was to measure the accuracy of the non-rigid registration technique and to compare it to a rigid registration technique. In the future, we believe our technique will enable better planning and improved placement of cryoablation applicators, which will lead to better tumor coverage and lower recurrence rates.

Both mean 95% HD and FRE values were lower, and mean DSC value was higher when using the non-rigid registration technique. The mean DSC value (0.96) obtained using our non-rigid registration technique was identical to the DSC reported for a similar non-rigid registration technique used to aid the assessment of regional renal function [15]. Our registration technique was just as accurate and was capable of fusing images from two

modalities, each obtained with the patient in different positions. In addition, 95%HD and FRE values were better than those reported by Wein et al. who used a non-rigid registration to fuse between CT and US images of the kidney [24]. Wein et al. used an automatic, real-time non-rigid registration technique to fuse pre-procedural contrast-enhanced CT images with intra-procedural US images prior to percutaneous biopsy or radio-frequency ablation of renal tumors; they achieved an FRE of 5.0 mm [24]. Our better results (FRE = 1.7 mm) may have been due to the use of a B-Spline registration step in addition to an initial affine registration that accounted for soft tissue deformation of the organ. Also, our use of cropped and masked data for the non-rigid registration technique may have helped. We believe a FRE value of 1.7 mm is sufficiently accurate to aid for a CT-guided percutaneous cryoablation procedure; an error of 1.7 mm is relatively small compared to most renal tumors that would be treated with cryoablation. When comparing this error to the image resolution, which was less then 0.6 mm for the CT images and 0.8 mm for the MR images, the error will thus span approximately two or three pixels in each of the images. We believe that higher resolution images may lead to improved registration errors; however, they will also require larger acquisition times for MR, and a change in the current clinical protocols.

Our non-rigid registration technique was used to fuse pre-procedural MR images to the initial intra-procedural CT images obtained to plan the cryoablation procedure. The same technique could be used to register pre-procedural MR images to the CT images obtained after all cryoablation applicators have been placed, allowing assessment of the location of the applicators in the tumor. Similarly, the pre-procedural MR images could be registered to the CT images obtained after freezing to assess coverage of the tumor by the iceball. In short, our non-rigid registration technique is practical for clinical use and can potentially offer three main advantages: more precise planning, accurate assessment of the location of the applicators in the tumor, and improved monitoring of the iceball.

One disadvantage of our registration technique is the time (15 min) required to perform it. The registration time limits its applicability to the planning stage of the procedure. The registration can be performed while the patient is being prepared and the interventional field sterilized, but our technique may not be suitable to register pre-procedural images to intra-procedural images while applicator placement or iceball monitoring due to long processing time. With reduced registration time, the technique can be applied during applicator placement or iceball monitoring. The current registration time included the time for segmentation of the kidney on the CT images, 1–3 min for manual pre-processing of the images (including cropping and masking) and 48.4 s computation time. Hence the largest part of the registration time was spent on segmentation of the kidney. Therefore, automated segmentation would help to reduce the registration time.

Our results point to the potential of a non-rigid registration technique to support CT-guided cryoablation procedures. However, there are some limitations to our study. The first limitation is that the initial segmentations of the kidney were performed using a semi-automatic segmentation method which required some minor manual correction. The manual correction was provided by only a single radiologist in this study and hence, inter- and intra-observer variability was not evaluated. However, inter- and intra-observer variability is likely to be low since the kidney is generally well-defined and easily distinguishable from surrounding retroperitoneal fat. Furthermore, in our previous study of deformable registration [25], we found that the inter- and intra-observer variability by DSC value in prostate segmentation presented a standard deviation of only 0.01. The impact of this variability, however, should not affect the statistical significance in comparing rigid and non-rigid registration if similar variability occurs in kidney segmentation. Therefore, we concluded that the impact of inter- and intra-observer variability is nominal in our study. The second limitation is that the study was retrospective and involved only 11 patients.

Although the non-rigid registration technique was significantly better than the rigid registration technique, a larger prospective study will need to be performed in which the non-rigid registration technique is used during the ablation procedure to assess the impact of the technique on clinical outcomes.

This method was designed to register pre-procedure contrast-enhanced MRI to intra-procedure unenhanced CT. Some centers use pre-procedure contrast-enhanced CT images for tumor visualization. In this sense, although MRI and CT are comparable in their ability to detect and characterize renal tumors, MRI provides better tumor to renal parenchymal contrast. MRI does not utilize ionizing radiation and MR images are generally used to follow the patient hence it is important to use MRI pre-procedurally. However, the technique is versatile and we believe it can be used with pre-procedural CT images, which has become the topic of future work.

Conclusions

We have described a non-rigid registration technique that can be used to fuse pre-procedural contrast-enhanced MR images and intra-procedural unenhanced CT images during CT-guided cryoablation of renal tumors. We have demonstrated that the non-rigid registration technique was more accurate than the rigid registration technique. This technique can be used to improve visualization of renal tumors during percutaneous CT-guided cryoablations. Our results suggest that a clinical trial is warranted.

Acknowledgments

This publication was made possible by Grant Number 5U41RR019703, 1R01CA124377, 5U54EB005149 from NIH. Its contents are solely the responsibility of the authors and do not necessarily represent the official views of the NIH. Part of this study was funded by Intelligent Surgical Instruments Project of METI (Japan). The abstract of this publication was awarded the RSNA 2009 Trainee Research Prize.

References

1. Shingleton WB, Sewell PE. Percutaneous renal tumor cryoablation with magnetic resonance imaging guidance. J Urol 2001;165(3):773–776. [PubMed: 11176465]
2. Bassignani MJ, Moore Y, Watson L, Theodorescu D. Pilot experience with real-time ultrasound guided percutaneous renal mass cryoablation. J Urol 2004;171(4):1620–1623. [PubMed: 15017235]
3. Gupta A, Allaf ME, Kavoussi LR, Jarrett TW, Chan DYS, Su LM, Solomon SB. Computerized tomography guided percutaneous renal cryoablation with the patient under conscious sedation: initial clinical experience. J Urol 2006;175(2):447–452. [PubMed: 16406968]
4. Atwell TD, Farrell MA, Leibovich BC, Callstrom MR, Chow GK, Blute ML, Charboneau JW. Percutaneous renal cryoablation: experience treating 115 tumors. J Urol 2008;179(6):2136–2140. [PubMed: 18423719]
5. Clark TWI, Millward SF, Gervais DA, et al. Reporting standards for percutaneous thermal ablation of renal cell carcinoma. J Vasc Interv Radiol 2006;17(10):1563–1570. [PubMed: 17056998]
6. Szolar DH, Kammerhuber F, Altziebler S, Tillich M, Breinl E, Fotter R, Schreyer HH. Multiphasic helical CT of the kidney: increased conspicuity for detection and characterization of small (<3-cm) renal masses. Radiology 1997;202(1):211–217. [PubMed: 8988213]
7. Berns AS, Kanter A, Cohen JJ, et al. Nephrotoxicity of contrast-media. Kidney Int 1989;36(4):730–740. [PubMed: 2681935]
8. Livraghi T, Solbiati L, Meloni MF, Gazelle GS, Halpern EF, Goldberg SN. Treatment of focal liver tumors with percutaneous radio-frequency ablation: complications encountered in a multicenter study. Radiology 2003;226(2):441–451. [PubMed: 12563138]

9. Goldberg SN, Gazelle GS, Mueller PR. Thermal ablation therapy for focal malignancy: a unified approach to underlying principles, techniques, and diagnostic imaging guidance. Am J Roentgenol 2000;174(2):323–331. [PubMed: 10658699]
10. Wells WM 3rd, Viola P, Atsumi H, Nakajima S, Kikinis R. Multi-modal volume registration by maximization of mutual information. Med Image Anal 1996;1(1):35–51. [PubMed: 9873920]
11. Giele ELW, de Priester JA, Blom JA, den Boer JA, van Engelshoven JMA, Hasman A, Geerlings M. Movement correction of the kidney in dynamic MRI scans using FFT phase difference movement detection. J Magn Reson Imaging 2001;14(6):741–749. [PubMed: 11747031]
12. Song T, Lee VS, Rusinek H, Kaur M, Laine AF. Automatic 4-D registration in dynamic MR renography based on over-complete dyadic wavelet and Fourier transforms. Med Image Comput Comput Assist Interv 2005;3750:205–213. [PubMed: 16685961]
13. de Senneville BD, Mendichovszky LA, Roujol S, Gordon I, Moonen C, Grenier N. Improvement of MRI-functional measurement with automatic movement correction in native and transplanted kidneys. J Magn Reson Imaging 2008;28(4):970–978. [PubMed: 18846555]
14. Rueckert D, Sonoda LI, Hayes C, Hill DLG, Leach MO, Hawkes DJ. Nonrigid registration using free-form deformations: application to breast MR images. IEEE Trans Med Imaging 1999;18(8): 712–721. [PubMed: 10534053]
15. Zoellner FG, Sancee R, Rogelj P, Ledesma-Carbayo MJ, Rorvik J, Santos A, Lundervold A. Assessment of 3D DCE-MRI of the kidneys using non-rigid image registration and segmentation of voxel time courses. Comput Med Imaging Graph 2009;33(3):171–181. [PubMed: 19135861]
16. Gervais DA, McGovern F, Arellano RS, McDougal WS, Mueller PR. Renal cell carcinoma: clinical experience and technical success with radio-frequency ablation of 42 tumors. Radiology 2003;226(2):417–424. [PubMed: 12563135]
17. Gering DT, Nabavi A, Kikinis R, et al. An integrated visualization system for surgical planning and guidance using image fusion and an open MR. J Magn Reson Imaging 2001;13(6):967–975. [PubMed: 11382961]
18. Lange T, Wenckebach TH, Lamecker H, et al. Registration of different phases of contrast-enhanced CT/MRI data for computer-assisted liver surgery planning: evaluation of state-of-the-art methods. Int J Med Robot Comput Assist Surg 2005;1(3):6–20.
19. Elhawary H, Oguro S, Tuncali K, et al. Intra-operative multimodal non-rigid registration of the liver for navigated tumor ablation. Med Image Comput Comput Assist Interv 2009;5761:837–844. [PubMed: 20426066]
20. Archip N, Clatz O, Whalen S, et al. Non-rigid alignment of pre-operative MRI, fMRI, and DT-MRI with intra-operative MRI for enhanced visualization and navigation in image-guided neurosurgery. Neuroimage 2007;35(2):609–624. [PubMed: 17289403]
21. West J, Fitzpatrick JM, Wang MY, et al. Comparison and evaluation of retrospective intermodality brain image registration techniques. J Comput Assist Tomogr 1997;21(4):554–566. [PubMed: 9216759]
22. Mount DM, Netanyahu NS, Le Moigne J. Efficient algorithms for robust feature matching. Pattern Recognit 1999;32(1):17–38.
23. Zou KH, Warfield SK, Bharatha A, et al. Statistical validation of image segmentation quality based on a spatial overlap index—Scientific reports. Acad Radiol 2004;11(2):178–189. [PubMed: 14974593]
24. Wein WG, Brunke S, Khamene A, Callstrom MR, Navab N. Automatic CT-ultrasound registration for diagnostic imaging and image-guided intervention. Med Image Anal 2008;12(5):577–585. [PubMed: 18650121]
25. Bharatha A, Hirose M, Hata N, et al. Evaluation of three-dimensional finite element-based deformable registration of pre- and intraoperative prostate imaging. Med Phys 2001;28(12):2551–2560. [PubMed: 11797960]

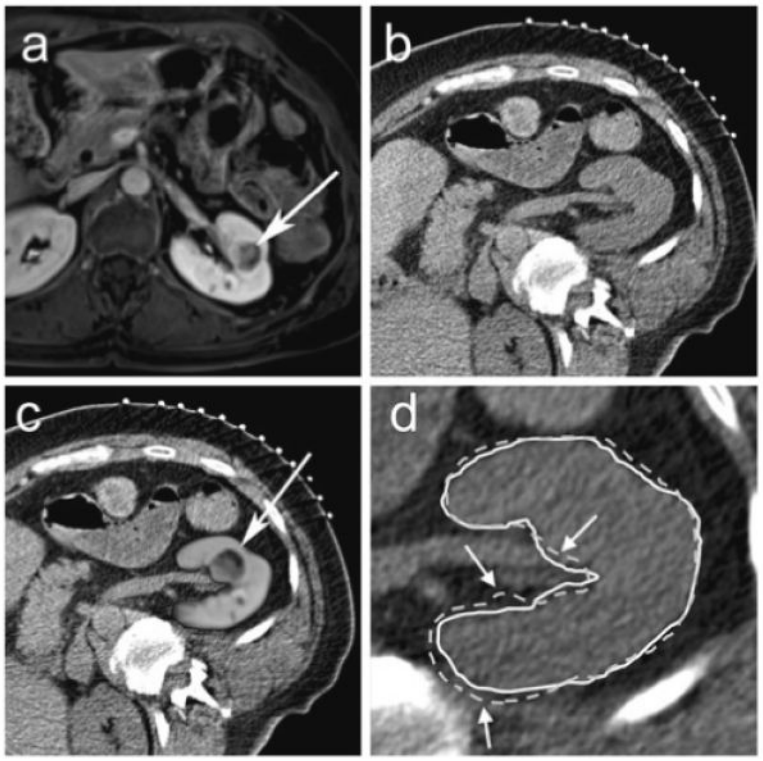

Fig. 1.

63-year-old female with left renal cell carcinoma. **a** Pre-procedural transverse contrast-enhanced spoiled gradient echo MR image of patient in supine position in a 1.5T scanner shows a 2.1 cm left renal mass (*arrow*). **b** Planning transverse unenhanced CT scan in the right posterior oblique position at the beginning of a CT-guided renal cryoablation shows the mass but the margins are not defined well. **c** MR image fused with CT image after non-rigid registration technique shows well-defined tumor in the left kidney (*arrow*). **d** The renal contour derived from registered MR images using non-rigid registration (*solid white line*) matches the renal contour on the CT image (*white arrows*) better than the renal contour derived from registered MR images using rigid registration (*dotted white line*)

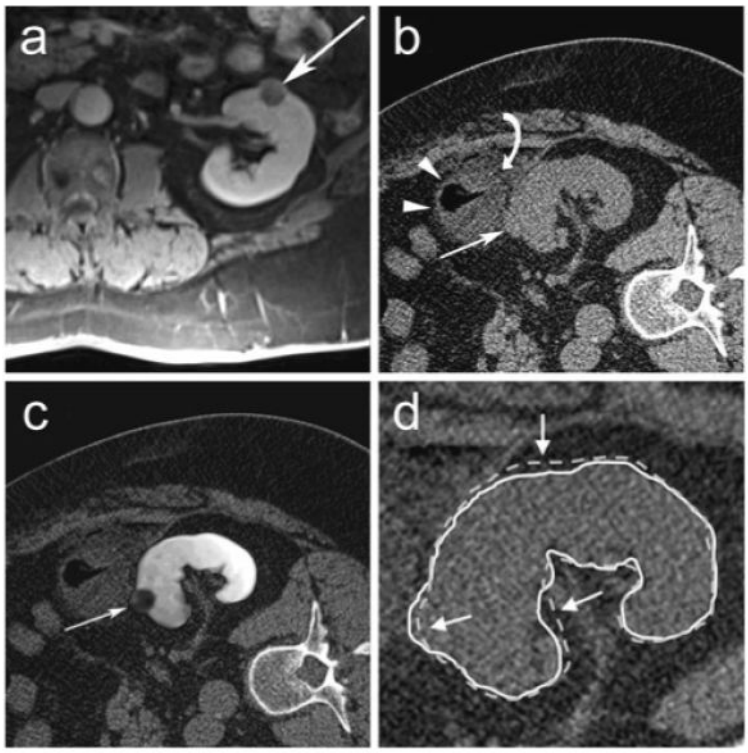

Fig. 2.

61-year-old male with left renal cell carcinoma. **a** Pre-procedural transverse contrast-enhanced spoiled gradient echo MR image of patient in supine position in a 1.5T scanner shows a 1.9 cm left renal mass (*arrow*). **b** Transverse unenhanced planning CT scan in the right lateral decubitus position shows exophytic portion of left renal mass (*arrow*) but the central extent of the tumor is not visible. The mass (*white arrow*) is obscured further by the colon (*white arrowheads*) and injected saline (*curved white arrow*) used to separate the colon from the mass. **c** MR image fused with CT image after non-rigid registration technique shows full extent of mass in the left kidney (*arrow*). **d** The renal contour derived from registered MR images using non-rigid registration (*solid white line*) matches the renal contour on the CT image (*white arrows*) better than the renal contour derived from registered MR images using rigid registration (*dotted white line*)

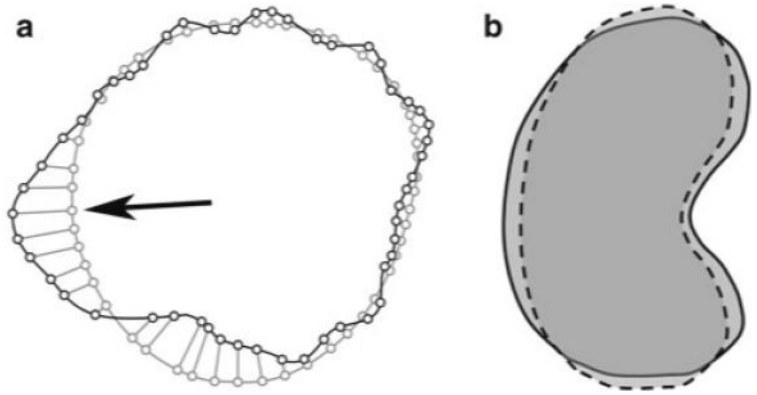

Fig. 3.

a Hausdorff Distance is the maximum perpendicular distance between closest points from two contours of registered images. *Black line* represents a renal contour from one image and *gray line* represents a renal contour from another registered image. *Small circles* represent corresponding closest points between each contour. Hausdorff distance represents the distance between *small circles* at *black arrow*. **b** Dice coefficient similarity (DSC) is an index of overlap of two different volumes. *Solid black line* represents a renal volume from one image and *dotted black line* represents a renal volume from another image after registration. DSC is always between 0 and 1; higher DSC indicates better match between the two different volumes

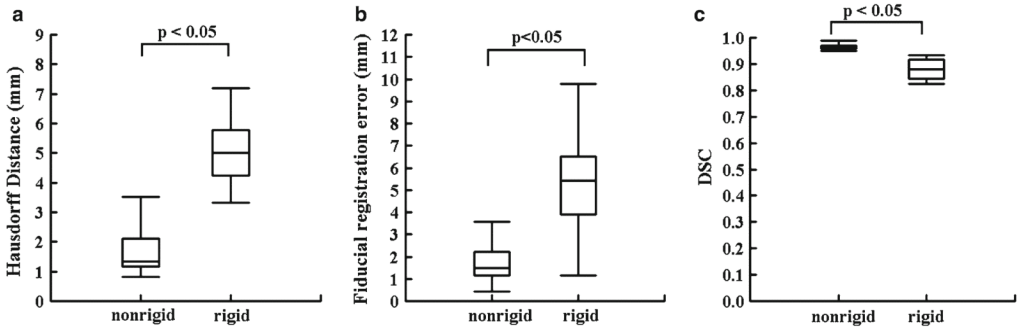

Fig. 4.

Boxplots of the 95% Hausdorff distance (HD), fiducial registration error (FRE), and Dice Similarity Coefficient (DSC) for non-rigid and rigid registration, techniques applied to pre-procedural MR and intra-procedural CT images (**a**, **b**, **c**). Median values with lower and upper quartile (*box*), 1.5 times the interquartile range (*whiskers*) are shown in each figure part